CHINESE JOURNAL OF PHYSICS VOL. 41 , NO. 6 DECEMBER 2003

Occurrence and Variation of Spin-State Transitions in $La_{1-x}Eu_xCoO_3$ Cobaltates

C. Y. Chang, B. N. Lin, and H. C. Ku

Department of Physics, National Tsing Hua University, Hsinchu, Taiwan 300, R.O.C.

Y. Y. Hsu

Institute of Physics, Academia Sinica, Taipei, Taiwan 115, R.O.C.

(Received June 9, 2003)

Structural, magnetic, and Co K-edge X-ray absorption near-edge structure (XANES) spectroscopic studies for the stoichiometric $La_{1-x}Eu_xCoO_3$ ($0 \leq x \leq 1$) system with trivalent Co^{3+} are reported. The thermally-excited spin-state transition from low-spin (LS) to intermediate-spin (IS) state increases from $T_s \sim 105$ K for $LaCoO_3$ ($x = 0$) to ~140 K for $x = 0.25$, to ~200 K for $x = 0.5$, and extrapolates to ~295 K for $EuCoO_3$ ($x = 1$), where the IS state is a mixture of d^6 ($t_{2g}^5 e_g^1$) and $d^7\underline{L}$ ($t_{2g}^5 e_g^2$ with a ligand hole) with filled t_{2g} majority spin states. The small pre-edge feature observed in room temperature XANES for the system in the IS state is from the $1s$-$3d$ quadrupole transition, which is weakly allowed through the hybridization of Co $4p$ states with $3d$ states of the neighboring Co atoms. For $LaCoO_3$, the pre-edge can be fitted using three Gaussian peaks with energy separations $\Delta E(P_2 - P_1) = 2.0$ eV and $\Delta E(P_3 - P_2) = 1.5$ eV, where P_1, P_2, and P_3 presumably correspond to the unfilled t_{2g} minority, e_g majority, and e_g minority spin states, respectively.

PACS numbers: 71.27.+a, 75.20.Hr, 78.70.Dm

I. INTRODUCTION

Rhombohedral $LaCoO_3$ perovskite (space group $R\overline{3}c$) with trivalent $Co^{3+}(3d^6)$ is unique, in that it is a nonmagnetic Mott insulator at low temperature but undergoes a gradual spin-state transition to a paramagnetic state near 90–100 K and then a metal-insulator transition above 500 K [1-17]. It remains highly controversial whether the spin-state transition is from a low-spin state (LS: t_{2g}^6, S = 0) to an intermediate-spin state (IS: $t_{2g}^5 e_g^1$, S = 1) or to a high-spin state (HS: $t_{2g}^4 e_g^2$, S = 2) [1-4].

Since the Co t_{2g} orbitals form a narrow band which can be easily localized, while e_g orbitals with strong hybridization with a neighboring oxygen $2p$ state form a broad band, the local-density approximation with on-site Coulomb repulsion (LDA+U) calculation shows that the IS state is energetically comparable to the LS state, but much more stable than the HS state, due to the larger Co-O $3d$-$2p$ hybridization as well as the orbital order effect [5]. The X-ray photoemission (XPS) and X-ray absorption (XAS) studies, using a cluster model calculation for the LS, IS, HS states, and mixtures, indicate that the ground state is a Co^{III} LS state with heavily mixed d^6 (t_{2g}^6) and $d^7\underline{L}$ ($t_{2g}^6 e_g^1$ with a ligand hole) character

due to *d-p* hybridization, and the thermal-induced spin-state transition is a gradual LS-IS transition [7]. The infrared studies indicate a local lattice distortion during the LS-IS transition arising from the dynamical Jahn-Teller effect [8].

For the stable orthorhombic $RCoO_3$ (R = Pr, Nd, Sm, Eu, Gd, Tb, Dy) cobaltates with crystal structure very close to rhombohedral $LaCoO_3$ [1, 2, 13-15, 18-20], a cobalt spin-state transition is expected to occur for all $RCoO_3$ compounds. However, ^{59}Co NMR studies show no spin-state transition for $RCoO_3$ (R = Pr, Nd, Sm, Eu) [13, 14]. On the contrary, infrared studies show a 220-K spin-state transition for $PrCoO_3$ and a 275-K transition for $NdCoO_3$ [15]. In order to avoid the complication in identifying the spin-state transition caused by the presence of the magnetic rare earth R^{3+} moments, a more suitable series of $La_{1-x}Eu_xCoO_3$ ($0 \leq x \leq 1$) with nonmagnetic Eu^{3+} ground state (total angular momentum J = 0) is selected for a systematic study in this work.

II. EXPERIMENTS

The samples with nominal composition $La_{1-x}Eu_xCoO_{3+\delta}$ (x = 0, 0.25, 0.5, 0.75, 1; $\delta \sim 0$) were synthesized by standard solid-state reaction. High-purity La_2O_3 (99.99 %), Eu_2O_3 (99.99 %) and Co_3O_4 (99.99 %) powders were thoroughly mixed and calcined at 900°C in air for 2 days with several intermediate regrindings. The calcined powders were then pressed into pellets and sintered at 1000°C in air for 1 day. In order to avoid chemical reaction with the alumina crucible, several pellets were stacked together, with the bottom one left out for actual measurements later. Clean sintered pellets were then annealed in air, flowing O_2, or Ar gas at 950°C to check the sample homogeneity, vacancy, impurity, and oxygen content. The O_2-annealed samples show signs of cation vacancy, with smaller unit cell volume, and the Ar-annealed samples show signs of anion vacancy, also with smaller unit cell volume, so the air-annealed samples were chosen for measurements. The oxygen content parameter $\delta \sim 0$ for air-annealed samples were crosschecked by comparing the X-ray diffraction, magnetic susceptibility, and Co K-edge XANES data.

The powder X-ray Rietveld analysis data were collected with a Rigaku Rotaflex 18-kW rotating anode diffractometer using graphite monochromatized Cu-K_α radiation with a scanning step of 0.02° (5 second counting time per step) in the 2θ range of 10-100°. A RIQAS refinement program was used with an inorganic crystal structure database (ICSD) and diffraction database (ICDD) [21].

The dc magnetic susceptibility and magnetization measurements were carried out with a Quantum Design 7-T MPMS or a 1-T μ-metal shielded $MPMS_2$ superconducting quantum interference device (SQUID) magnetometer from 2 K to 300 K.

The X-ray absorption near-edge structure (XANES) measurements were performed at the Synchrotron Radiation Research Center (SRRC) in Taiwan. The Co K-edge XANES transmission mode data were collected at room temperature using the BL17C wiggler beamline with an X-ray photon energy range of 4-15 keV and energy resolution $E/\Delta E = 7000$. The photon energy was calibrated using a Co metal foil.

TABLE I: Hexagonal-axis ($R\bar{3}c$, Z = 6) lattice parameters a, c, and formula unit volume $V_{f.u.} = V_h/6$ for rhombohedral $LaCoO_3$ and orthorhombic (Pbnm, Z = 4) lattice parameters a, b, c, and formula unit volume $V_{f.u.} = V_0/4$ for $La_{1-x}Eu_xCoO_{3+\delta}$ ($0 \leq x \leq 1$; $\delta \sim 0$), spin-state transition temperature T_s, and room temperature molar magnetic susceptibility χ_m(300K).

Compound	a(Å)	b(Å)	c(Å)	Z	$V_{f.u}$(Å^3)	T_s(K)	χ_m(2K)[1] (cm^3/mol)	χ_m(300K)[1] (cm^3/mol)
$LaCoO_3$	5.4398(5)	—	13.0871(9)	6	55.91(2)	105	2.9×10^{-3}	3.1×10^{-3}
$La_{0.75}Eu_{0.25}CoO_3$	5.4246(5)	5.3580(5)	7.5986(7)	4	55.21(2)	140	3.8×10^{-3}	3.4×10^{-3}
$La_{0.5}Eu_{0.5}CoO_3$	5.3663(5)	5.3596(5)	7.5712(7)	4	54.44(2)	200	5.0×10^{-3}	4.0×10^{-3}
$La_{0.25}Eu_{0.75}CoO_3$	5.3134(5)	5.3650(5)	7.5263(7)	4	53.64(2)	245*	6.6×10^{-3}	4.3×10^{-3}
$EuCoO_3$	5.2600(5)	5.3698(5)	7.4813(7)	4	52.83(2)	295*	8.4×10^{-3}	5.8×10^{-3}

*Linear fit extrapolation; [1]Applied field B_a = 3 T.

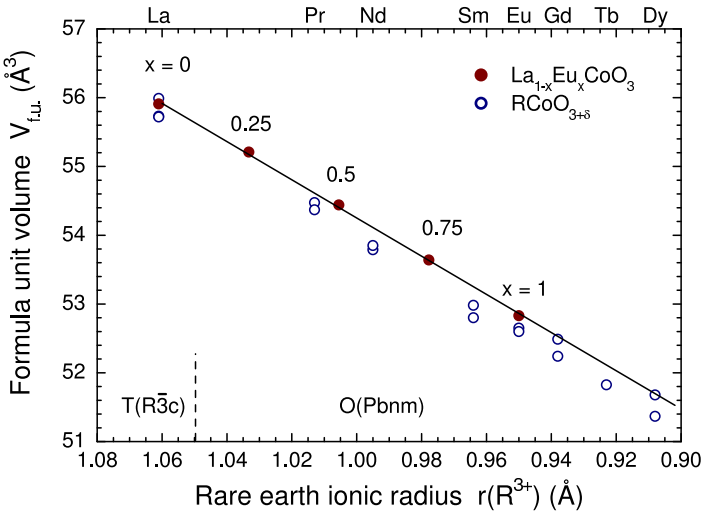

FIG. 1: Variation of formula unit volume $V_{f.u.}$ with average rare earth ionic radius $r(R^{3+})$ for the stoichiometric $La_{1-x}Eu_xCoO_3$ (x = 0, 0.25, 0.5, 0.75, 1: solid circles) system and $RCoO_{3+\delta}$ (R = La, Pr, Nd, Sm, Eu, Gd, Tb or Dy; $\delta \geq 0$: open circles) system.

III. RESULTS AND DISCUSSION

The rhombohedral phase is stable only in $LaCoO_3$ with hexagonal-axis lattice parameters a = 5.4398 Å and c =13.0871 Å (formula unit Z = 6), due to a large La^3+ ionic radius of 1.061 Å, and can be easily transformed into the orthorhombic phase (space group Pbnm with formula unit Z = 4) with smaller Eu^{3+} (ionic radius 0.95 Å) substitution. The hexagonal lattice parameters a, c, and formula unit volume $V_{f.u.} = V_h/6$ for rhombohedral $LaCoO_3$, as well as the orthorhombic lattice parameters a, b, c, and $V_{f.u.} = V_0/4$ for $La_{1-x}Eu_xCoO_3$ (x = 0.25, 0.5, 0.75, 1), are listed in Table I. The variation of $V_{f.u.}$ with av-

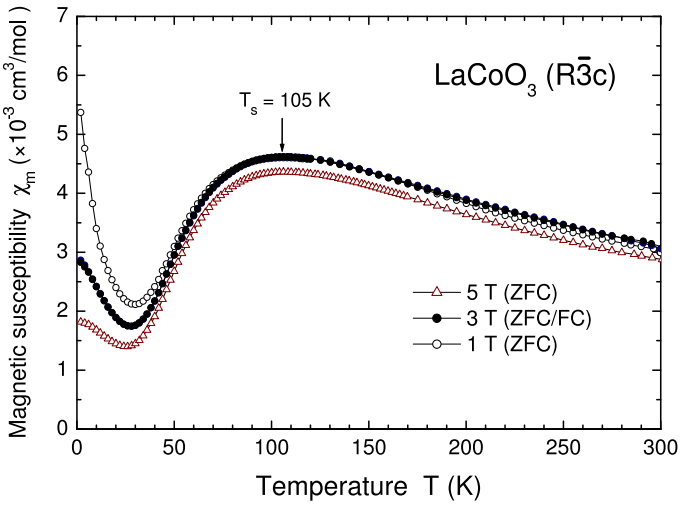

FIG. 2: Temperature dependence of the molar magnetic susceptibility $\chi_m(T)$ in the 1-T, 3-T, and 5-T zero-field-cooled (ZFC) and 3-T field-cooled (FC) mode for rhombohedral $LaCoO_3$.

erage rare earth ionic radius r(R^{3+}) for $La_{1-x}Eu_xCoO_3$, along with the reported $RCoO_{3+\delta}$ (R = La, Pr, Nd, Sm, Eu, Gd, Tb, Dy) data are shown in Fig. 1 [4, 11, 12, 18-20]. The structural studies have shown that there is no oxygen interstitial site for $RCoO_{3+\delta}$. With fully occupied oxygen sublattice and R/Co cation vacancies, the correct crystallographic composition is $R_zCo_zO_3$ with $z = 3/(3+\delta)$, and a maximum formula unit volume is achieved at the stoichiometric composition $RCoO_3$. From Fig. 1, it is clear that $La_{1-x}Eu_xCoO_{3+\delta}$ with large formula unit volumes are very close to the stoichiometric $\delta \sim 0$ composition with trivalent Co^{3+}. The $V_{f.u.}$ in $La_{1-x}Eu_xCoO_3$ decreases monotonically with decreasing average rare earth radius r. This indicates a stronger octahedral CoO_6 crystal field splitting energy Δ_{cf} with progressive Eu substitution.

The temperature dependence of the molar magnetic susceptibility $\chi_m(T)$ in applied fields of 1-T, 3-T, and 5-T for the rhombohedral $LaCoO_3$ and the orthorhombic $La_{0.75}Eu_{0.25}CoO_3$ are shown in Fig. 2 and Fig. 3, respectively. For $LaCoO_3$, as in the previous reported data, χ_m decreases abruptly around 105 K, and is accompanied by a weak Curie-Weiss contribution below 30 K [7, 8]. The gradual LS-IS transition temperature T_s ~105 K, defined as the local magnetic susceptibility maximum, is fairly field independent. At 3 T, the field-cooled (FC) and zero-field-cooled (ZFC) curves are almost identical, with a low $\chi_m(2\,\mathrm{K})$ of 2.9×10^{-3} cm^3/mol, which is close to the reported single crystal value [8]. The low temperature magnetic susceptibility is field-dependent and $\chi_m(2\,\mathrm{K})$ decreases to 1.8×10^{-3} cm^3/mol at 5 T. The magnetization measurement at 5 K yields a weak ferromagnetic hysteresis loop with a small saturation magnetic moment m_s of $1.6\times10^{-2}\mu_B$/Co at 5 T. This weak ferromagnetic contribution is most likely attributed to magnetic impurities. However, since the LS state is a Co(III) state with heavily mixed d^6 (t_{2g}^6) and $d^7\underline{L}$ ($t_{2g}^6e_g^1$ with a ligand hole), the ground state is not completely nonmagnetic with S = 0. On

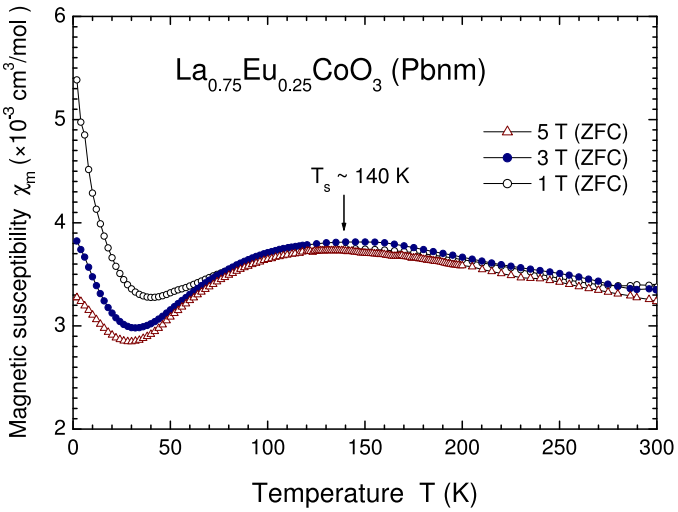

FIG. 3: Temperature dependence of the molar magnetic susceptibility $\chi_m(T)$ in the 1-T, 3-T, and 5-T ZFC modes for orthorhombic $La_{0.75}Eu_{0.25}CoO_3$.

the contrary, the room temperature magnetic susceptibility in the paramagnetic IS state with heavily mixed d^6 ($t_{2g}^5 e_g^1$) and $d^7\underline{L}$ ($t_{2g}^5 e_g^2$ with a ligand hole) is fairly field independent with $\chi_m(300\,\mathrm{K}) \sim 3{\times}10^{-3}$ cm^3/mol.

For Eu-doped $La_{0.75}Eu_{0.25}CoO_3$, a higher LS-IS transition of $T_s \sim 140$ K is detected with a smaller formula unit volume $V_{f.u}$ of 55.21 Å^3 for $x = 0.25$, as compared with 55.91 Å^3 for $x = 0$. Since the LS ground state and LS-IS transition for the cobaltates originate from the competition between the crystal-field energy Δ_{cf} and the intra-atomic Hund's rule exchange energy Δ_{ex}, the higher T_s is apparently due to a stronger t_{2g}-e_g splitting in the CoO_6 octahedral crystal field, with larger crystal-field splitting energy Δ_{cf} at $x = 0.25$ with smaller formula unit volume.

The molar magnetic susceptibility $\chi_m(T)$ data at 3 T for the $La_{1-x}Eu_xCoO_3$ (x = 0, 0.25, 0.5, 0.75, 1) system are shown in Fig. 4. The spin-state transition temperature T_s increases from 105 K for $x = 0$, to 140 K for $x = 0.25$, and 200 K for $x = 0.5$. For x = 0.75 and 1, the intrinsic signal is masked by the magnetic signal of Eu^{3+} excited state (J = 1). The increase of the room temperature magnetic susceptibility, from $3.1{\times}10^{-3}$ cm^3/mol for $x = 0$ to $5.8{\times}10^{-3}$ cm^3/mol for $x = 1$, is attributed to the Eu magnetic signal. The increase of the low temperature $\chi_m(2\,\mathrm{K})$ from $2.9{\times}10^{-3}$ cm^3/mol for $x = 0$ to $8.4{\times}10^{-3}$ cm^3/mol for $x = 1$, is also due to the same cause.

The variation of T_s with formula unit volume $V_{f.u.}$ is shown in Fig. 5. A simple linear fit to smaller volume leads to an extrapolated value $T_s \sim 245$ K, for $x = 0.75$ with $V_{f.u.}$ = 53.84 Å^3, and ~295 K, for $EuCoO_3$ with $V_{f.u.} = 52.83$ Å^3. Generalizing the same argument to other magnetic rare earth cobaltates $RCoO_3$ (R = Pr, Nd, Sm, Gd, Tb, Dy) with smaller formula unit volume (Fig. 1), all compounds should undergo a spin-state transition in the magnetic measurement, if not screened by the strong rare earth R^{3+} magnetic signal. On

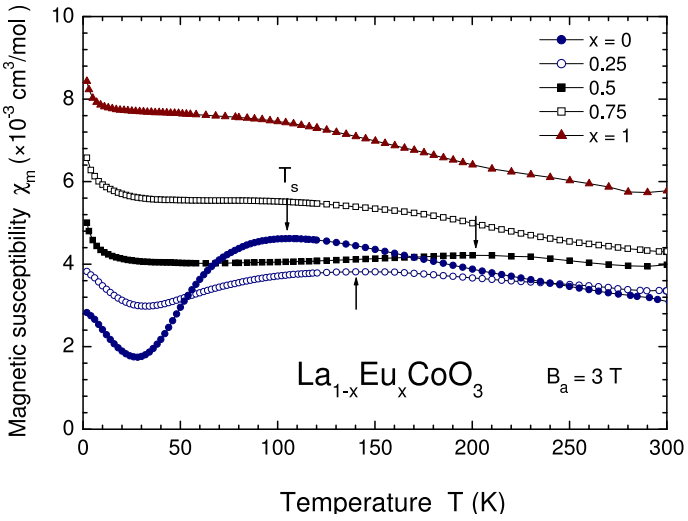

FIG. 4: Temperature dependence of the molar magnetic susceptibility $\chi_m(T)$ in the 3-T ZFC mode for $La_{1-x}Eu_xCoO_3$ (x = 0, 0.25, 0.5, 0.75, 1).

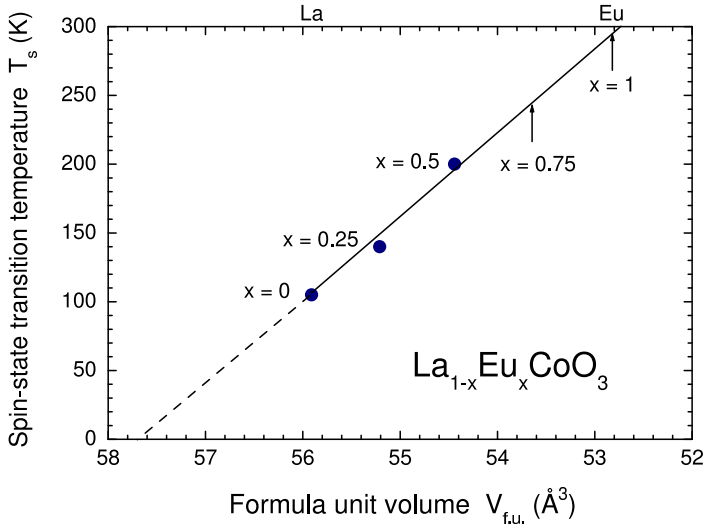

FIG. 5: Variation of the spin-state transition temperature T_s with formula unit volume $V_{f.u.}$ for $La_{1-x}Eu_xCoO_3$ (x = 0, 0.25, 0.5, 0.75, 1).

the other end, the extrapolated $T_s = 0$ K for larger formula unit cell $V_{f.u.} > 57.7$ Å^3 with much weaker crystal-field energy Δ_{cf} can explain the appearance of an antiferromagnetic ground state for the isostructural $La_{1-x}Eu_xMnO_3$ system with $V_{f.u} > 58.3$ Å^3 [22].

The normalized Co K-edge XANES structure at room temperature for $La_{1-x}Eu_xCoO_3$ (x = 0, 0.25, 0.5, 1) in the intermediate state is shown in Fig. 6. The energy is calibrated by using a Co metal foil with threshold energy of E_0 = 7709 eV at

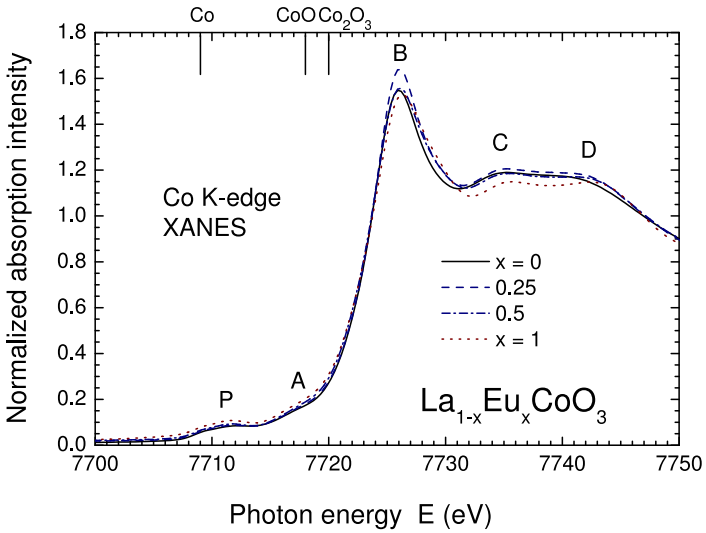

FIG. 6: Co K-edge XANES for $La_{1-x}Eu_xCoO_3$ (x = 0, 0.25, 0.5, 1). The threshold edge energy of two standards (CoO, Co_2O_3) and Co metal foil are also indicated.

the inflection point of the edge. The E_0 for the two standards CoO (Co^{2+}) and Co_2O_3 (Co^{3+}) indicates a substantial shift of the edge energy with increasing Co formal valence. The almost identical threshold edge energy $E_0 \sim 7720$ eV for the $La_{1-x}Eu_xCoO_3$ system indicates that all samples are very close to the stoichiometric composition with trivalent Co^{3+}.

The K-edge XANES main edge absorption is attributed to the 1s-4p dipole transition to the Co 4p states. Since the crystal structure of the $La_{1-x}Eu_xCoO_3$ system is similar to that of the $LaMnO_{3+\delta}$ system (orthorhombic for $\delta \leq 0.025$ and rhombohedral for $\delta > 0.025$) system, the shape of the edge is similar to the K-edge XANES of $LaMnO_{3+\delta}$ [23, 24]. The main edge features, labeled as A, B, C, and D, can thus be reasonably explained by the Co 4p partial density of states, their broadening reflects the finite lifetime of the 1s core hole [23]. Feature A is attributed to the hybridization between the Mn 4p states with the rare earth La/Eu orbitals, feature B is the Mn 4p states split by the crystal field and feature C and D are the MnO_6 octahedron surrounded by eight La/Eu atoms. The Co 4p states, like the Mn 4p states, are highly delocalized and extend over several Co atoms [23]. The small pre-edge feature P observed corresponds to the 1s-3d quadrupole transition, which is weakly allowed through the hybridization of Co 4p states with 3d states of neighboring Co atoms [23, 24].

Fig. 7 shows the low intensity pre-edge P feature for $La_{1-x}Eu_xCoO_3$ in the IS state. The pre-edge can be fitted with three Gaussian peaks P_1, P_2, and P_3, after having the smooth background subtracted. For $LaCoO_3$ (inset), the energy separations are $\Delta E(P_2 - P_1) = 2.0$ eV and $\Delta E(P_3 - P_2) = 1.5$ eV. For comparison, energy separations $\Delta E(P_2 - P_1) = 2.0$ eV and $\Delta E(P_3 - P_2) = 1.3$ eV are derived for $EuCoO_3$. The thermally excited IS state is in the mixture of d^6 ($t_{2g}^5 e_g^1$) and $d^7\underline{L}$ ($t_{2g}^5 e_g^2$ with a ligand hole) due to a strong hybridization

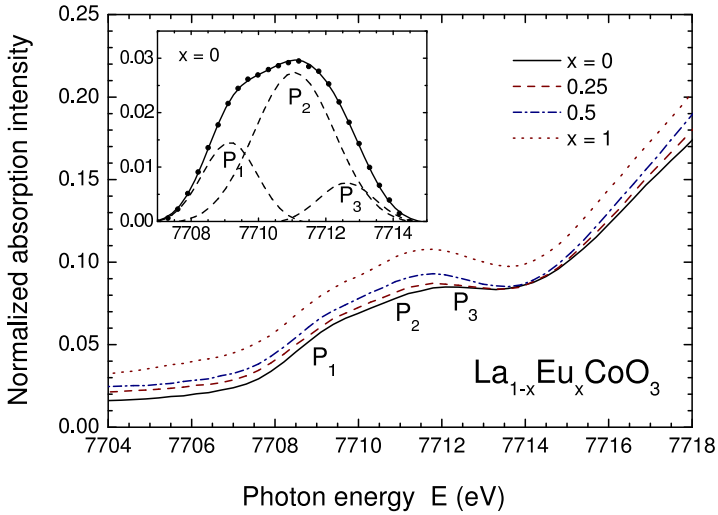

FIG. 7: Low intensity pre-edge region of Co K-edge XANES for $La_{1-x}Eu_xCoO_3$ (x = 0, 0.25, 0.5, 1). The pre-edge P can be fitted with three peaks P_1, P_2, and P_3 (inset for $LaCoO_3$).

of the e_g electrons with oxygen $2p$ orbials. The electronic configuration is $t_{2g}^5\sigma^*$ with narrow t_{2g} bands and a broader σ^* band [5]. The LDA+U calculation for $LaCoO_3$ in the IS state implies that the allowed $1s$-$3d$ dipole transition goes into the unfilled t_{2g} and e_g states [5]. With larger $\Delta E(P_2 - P_1)$ and smaller $\Delta E(P_3 - P_2)$, the three peaks P_1, P_2, and P_3 presumably correspond to the unfilled t_{2g} minority, e_g majority, and e_g minority spin states, respectively.

IV. CONCLUSION

The spin-state transition temperature T_s from low-spin (LS) to intermediate-spin (IS) increases from ∼105 K for $x = 0$ ($LaCoO_3$), to ∼140 K for $x = 0.25$, ∼200 K for $x = 0.5$ and is extrapolated to ∼295 K for $x = 1$ ($EuCoO_3$). The small pre-edge feature observed in room temperature XANES is from the $1s$-$3d$ quadrupole transition, which is weakly allowed through the hybridization of Co $4p$ states with the $3d$ states of neighboring Co atoms. For $LaCoO_3$ in the IS state, the pre-edge can be fitted using three peaks with energy separation $\Delta E(P_2 - P_1) = 2.0$ eV and $\Delta E(P_3 - P_2) = 1.5$ eV, where the three peaks P_1, P_2, and P_3 presumably correspond to the unfilled t_{2g} minority, e_g majority, and e_g minority spin sates, respectively.

Acknowledgments

This work was supported by the National Science Council of the R.O.C. under contract Nos. NSC91-2119-M007-005, 2112-M007-060.

References

[1] W. C. Koehler and E. O. Wollan, J. Phys. Chem. Solids **2**, 100 (1957).
[2] J. B. Goodenough, J. Phys. Chem. Solids **6**, 287 (1958).
[3] M. Abbate, J. C. Fuggle, A. Fujimori, L. H. Tjeng, C. T. Chen, R. Potze, G. A. Sawatzky, H. Eisaki, and S. Uchida, Phys. Rev. B **47**, 16214 (1993), and references cited therein.
[4] M. A. Senaris-Rodriguez and J. B. Goodenough, J. Solid State Chem. **116**, 224 (1995), and references cited therein.
[5] M. A. Korotin, S. Yu. Ezhov, I. V. Solovyev, V. I. Anisimov, D. I. Khomskii, and G. A. Sawatzky, Phys. Rev. B **54**, 5309 (1996).
[6] E. Iguchi, K. Ueda, and W. H. Jung, Phys. Rev. B **54**, 17431 (1996).
[7] T. Saitoh, T. Mizokawa, A. Fujimori, M. Abbate, Y. Takeda, and M. Takano, Phys. Rev. B **55**, 4257 (1997).
[8] S. Yamaguchi, Y.Okimoto, and Y. Tokura, Phys. Rev. B **55**, R8666 (1997).
[9] Z. Y. Wu, M. Benfatto, M. Pedio, R. Cimino, S. Mobilio, S. R. Barman, K. Maiti, and D. D. Sarma, Phys. Rev. B **56**, 2228 (1997).
[10] K. Asai, A. Yoneda, O. Yokokura, J. M. Tranquada, G. Shirane, and K. Kohn, J. Phys. Soc. Jpn. **67**, 290 (1998).
[11] P. Ravindran, P. A. Korzhavyi, H. Fjellvag, and A. Kjekshus, Phys. Rev. B **60**, 16423 (1999).
[12] P. Porta, S. de Rossi, M. Faticanti, G. Minelli, I. Pettiti, L. Lisi, and M. Turco, J. Solid State Chem. **146**, 291 (1999).
[13] M. Itoh, M. Mori, S. Yamaguchi, and Y. Tokura, Physica B **259-261**, 902 (1999).
[14] M. Itoh, J. Hashimoto, S. Yamaguchi, and Y. Tokura, Physica B **281-282**, 510 (2000).
[15] L. Sudheendra, Md. M. Seikh, A. R. Raju, and C. Narayana, Chem. Phys. Lett. **340**, 275 (2001).
[16] O. Toulemonde, N. N'Guyen, F. Studer, and A. Traverse, J. Solid State Chem. **158**, 208 (2001).
[17] J. Androulakis, N. katsarakis, and J. Giapintzakis, Phys. Rev. B **64**, 174401 (2001).
[18] X. Liu and C. T. Prewitt, J. Phys. Chem. Solids, **52**, 441 (1991).
[19] Y. Y. Kim, D. H. Lee, T. Y. Kwon, and S. H. Park, J. Solid State Chem. **112**, 376 (1994).
[20] PCPDFWIN database, JCPDS-International Centre for Diffraction Data (1997).
[21] RIQAS program, Materials Data Inc., Livermore CA, USA (1996).
[22] C. T. Chen, B. N. Lin, Y. Y. Hsu, J. D. Liao, W. H. Cheng, J. Y. Lin, H. C. Ku, J. F. Lee, L. Y. Jang, and D. G. Liu, Phys. Rev. B, in press (2003).
[23] I. S. Elfimov, V. I. Anisimov, and G. A. Sawatzky, Phys. Rev. Lett. **82**, 4264 (1999).
[24] F. Bridges, C. H. Booth, G. H. Kwei, J. J. Neumeier, and G. A. Sawatzky, Phys. Rev. B **61**, 9237 (2000).